

Short Racetrack Windings for the Mechanical Characterization of Ceramic-Insulated Cables

Pierre Manil, and Françoise Rondeaux

Abstract— Electrical insulation is a key element in high field magnets design. The use of Nb_3Sn , winded before reaction and then thermally treated to obtain the superconducting intermetallic compound, supposes to adapt the insulation process. CEA/IRFU (FR) is investigating the possibility of using a ceramic electrical insulation that follows the same thermal cycle than the superconductor. This ceramic insulation would make it possible to get rid of the impregnation process.

The mechanical characterization of the ceramic-insulated cables is mandatory for the magnet designers. The increase of the Lorentz forces supposes to raise subsequently the characterization pressures, within the limits of the available press. An option to reach higher pressures with the same press is to reduce the sample surface by reducing its length. But approaching the twist pitch value, this can cause parasite effects such as sample untwisting, insulation cracks and boundary effect influence raise. Those effects appear to be particularly damaging in the case of ceramic insulation which is brittle.

To address these problems, the use of short racetrack windings is proposed for characterization. The behavior of dummy copper cable with this ceramic insulation is studied till up to 150 MPa with such samples, at room temperature, in the stack direction.

Index Terms— Ceramics, compression tests, electrical insulation, mechanical characterization, short racetrack windings.

I. INTRODUCTION

IF Nb_3Sn is today considered as the best low-temperature superconductor for high field magnets above 10 Tesla (T), its implementation remains delicate. After heat treatment, this material becomes brittle and strain-sensitive. As a consequence, most of the Nb_3Sn coils are produced following the “wind & react” sequence: the conductor is wound before being heat-treated at high temperature. This technique excludes the use of electrical insulators containing organic materials. After heat treatment, the coil is usually transferred into a mould to be vacuum-impregnated with epoxy resin. The transfer and the vacuum impregnation are time-taking and risky operations. To avoid these problems, we have developed a full ceramic insulation which is directly deposited on the un-reacted cable [1], [2]. It can follow the same thermal cycle

than the superconductor and supposes no impregnation.

Previous studies have shown that the intrinsic properties of the wire (critical current, residual resistivity ratio) are not affected by the process [1]-[3]. Furthermore, small Nb_3Sn strand solenoids insulated with this process have been built and tested successfully in high external magnetic fields up to 12 T. Stresses around 65 MPa in compression and 30 MPa in tension have been reached inside the coil. This ceramic insulation has not shown any failure, either electrical or mechanical. The quench current performances have shown no sign of degradation after several quenches [3], [4].

Following these encouraging results, the next step is to reach the stress levels expected in accelerator magnets on insulated cables (at least 150 MPa). This work has been started through mechanical compression tests at room temperature and at 4.2 K. The tests have been performed on ten or eight-stack samples and have highlighted experimental problems. Some preliminary mechanical results have been reported in [5].

II. SAMPLE DESIGN

A. Preliminary Observations

Several weak points of the stacks have been observed. First, the bare cable plasticity causes large sample deformation when there is no impregnation. Because of the short length of the stacks, there is an additional risk of cable untwisting. Those effects are particularly damaging with the Nb_3Sn and the ceramic insulation, which are brittle and very sensitive to local strains. For these reasons, it is not desirable to reduce the sample length L too much. L should be significantly longer than a cable twist pitch p (we consider $L > 1.5 p$).

On the other hand, for a fixed force, the pressure limit derives from the sample surface Σ , which is proportional to L . Designing new samples with a smaller surface would make the available pressure higher, for a given press.

B. Sample Geometry

Following these remarks, a new sample design is proposed for the compression tests. It consists in a short monolayer racetrack winding. First, the cable is wrapped with a mineral tape coated with our un-reacted ceramic precursor. The insulated cable is wound around a stainless steel pole as for real magnets. The winding tension increases the mechanical cohesion of the sample, and bonds the turns together. The number of turns N_t is fixed to five in order to have ten conductors under compression in total as for the ten-stacks.

Manuscript received 19 October 2009.

P. Manil is with CEA Saclay/IRFU/SIS, 91191 Gif-sur-Yvette, France (phone: +33-1 69 08 74 79; e-mail: pierre.manil@cea.fr).

F. Rondeaux is with CEA Saclay/IRFU/SACM, 91191 Gif-sur-Yvette, France (e-mail: francoise.rondeaux@cea.fr).

Fig. 1 represents the sample shape and introduces the geometrical parameters. The sample has only two free ends, reducing the untwisting. In this context, we believe we can reduce the straight section length L_{ss} , which is arbitrarily fixed to p . The cable lead end is clamped to the pole inside a tailored groove equipped with a screw. The other end is free. The pole half-width r has been fixed to 15 mm after bending tests. We wanted r to be as small as possible to have a compact sample. The sample is maintained between two clamps by threaded rods. Doing this, we make sure that the cable winding tension and the compressive pre-stress are retained during all the manufacturing and handling phases. During the compression test, the central pole is left in position. In the direction of compression, this configuration is comparable to the stacking of a ten-stack and a thick steel shim. But contrary to a stack, the racetrack sample is constrained longitudinally.

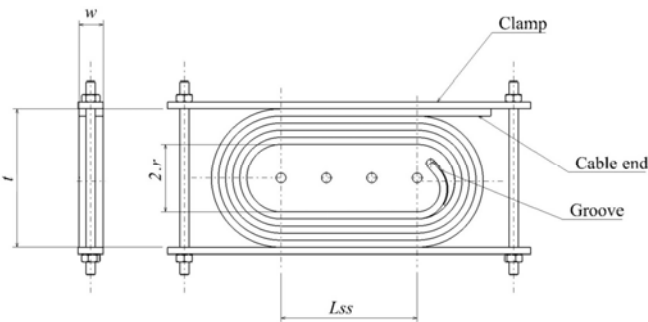


Fig. 1. Schematic sketch of the racetrack sample geometry.

The following study is led with dummy copper cable based of the NED properties specified in [6]. Further studies should be led with the real Nb_3Sn cable later. Dimensional constraints are imposed by the cable, the reaction furnace and the press. The sample parameters are listed in Table I.

TABLE I. SHORT RACETRACK SAMPLE PROPERTIES

Parameter	Symbol	Unit	Value
Number of strands	N_{str}	/	14
Strand diameter	ϕ_{str}	mm	1.25
Twist pitch	p	mm	60
Cable width	w_{cbl}	mm	9.7
Cable thickness at 20 MPa	t_{cbl}	mm	2.20
Insulation thickness per face (± 0.04 mm)	t_{ins}	mm	0.46
Number of turns	N_t	/	5
Pole half-width	r	mm	15
Straight section length	L_{ss}	mm	60

C. Sample Realization

As for most of the real Nb_3Sn magnets, the fabrication process follows a “wind and react” sequence. The winding is performed with the specific tooling represented in Fig. 2. At the end of the operation, the racetrack is clamped and the cable end is cut. The sample is placed in the heat treatment mould represented in Fig. 3 before being pre-stressed under a

press with pressures around 30 MPa. The pre-stress improves the sample cohesion after reaction. Its value has been experimentally adjusted during precedent campaigns. The sample follows a one-step thermal cycle: 60 °C/h up to 650 °C, then 50 h at 650 °C, under argon flow. This sequence is optimized for the NED cable [6], and is considered as an input in this study, even if dummy copper cable is used.

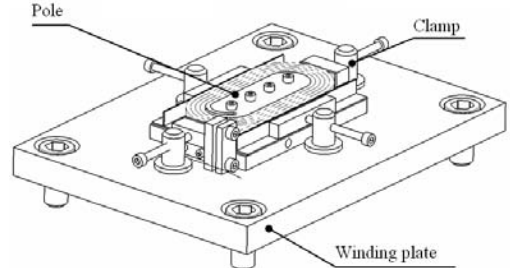


Fig. 2. Schematic view of the racetrack sample winding tooling.

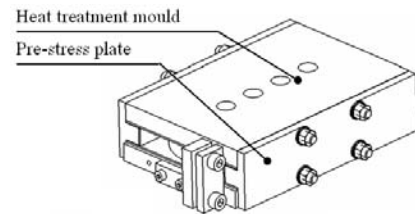


Fig. 3. Schematic view of the racetrack sample pre-stress and reaction mould.

III. COMPRESSIVE TESTS

A. Experimental Scheme

The idea of this first test campaign is to compare the results obtained with ten-stacks and racetrack samples. The samples widths are imposed by the cable parameters. Three geometries are considered, using the same dummy copper cable, with or without ceramic insulation:

- Short ten-stacks (S) with $L < p$;
- Long ten-stacks (L) with $L > p$;
- short Racetracks (R).

Table II gives the sample features at the beginning of the test.

TABLE II. SAMPLES DESCRIPTION

Name	Type	Insulation	L_{theo} (mm)	w_{theo} (mm)	Σ_0 (mm ²)	Pre-stress (MPa)	t_0 (mm)
SI1	S	ceramic	50	10.6	531	29.5	24.4
LN1	L	none	100	9.7	970	48.5	21.4
LI1	L	ceramic	100	10.6	1062	29.5	24.6
LI2	L	ceramic	100	10.6	1062	29.5	24.7
RN1	R	none	60	9.7	582	33.7	51.6
RI1	R	ceramic	60	10.6	637	30.8	54.7
RI2	R	ceramic	60	10.6	637	30.8	55.4

L_{theo} and w_{theo} are the theoretical length and width. For racetrack samples, $L_{theo} = L_{ss}$. The theoretical initial contact surface Σ_0 is equal to L_{theo} multiplied by w_{theo} . The pre-stress values before heat treatment are estimated on the base of Σ_0 . t_0 is the measured initial thickness, in the stack direction.

B. Procedure

The samples are inserted inside a compression mould. For the ten-stacks, the absence of a pole is compensated by a 30 mm-thick steel shim. The tests are carried out with a screw-

driven machine, which allows a compressive load up to 300 kN. All tests are performed at room temperature. The direction of the compression is perpendicular to the stacking. The deformations are measured by two symmetrical extensometers. Fig. 4 shows the experimental setup with *LNI*.

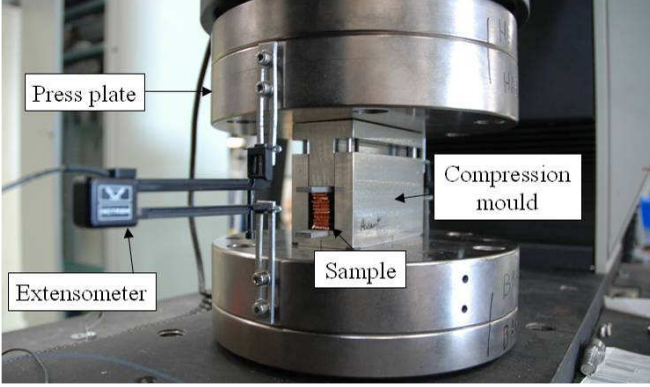


Fig. 4. Experimental setup during the test of the sample *LNI*.

The samples are submitted to a series of two cycles of uniaxial compression from a minimal force (corresponding to ~5 MPa) to the target force (corresponding successively to ~10, 20, 50, 75, 100, and 150 MPa). The compression speed is 0.2 mm/min. The equivalent pressures are estimated for each sample on the base of the initial contact surface Σ_0 . To evaluate the stress repartition on this surface, FUJI™ Prescale film is used. This pressure-measuring film is calibrated to change color gradually from white to red in a given stress range. Two layers of different sensitivity are superimposed: one calibrated for 10 to 50 MPa, the other for 130 to 300 MPa. The former will define the effective contact surface at the end of the test; the latter will help identify the peak stress zones.

A preliminary test is performed on the steel pole in the compression mould. The aim is to evaluate the stiffness of the support structure (pole + mould + press) without conductor. The equivalent compressive modulus E_s is estimated around 85 GPa. This corrective factor includes the steel stiffness as well as the compressibility of the press itself.

C. Post-Treatment

The test outputs are the press force F and the lateral extensions δ_L and δ_R versus time. Next calculations are based on the average extension $\delta = (\delta_L + \delta_R) / 2$.

The characteristic curve $\delta(F)$ is linearized section by section. The equivalent compressive modulus E_{tot} of the assembly (sample + support) is given in linear regime by (1):

$$E_{tot} = K_{lin} \cdot \frac{t_0}{\Sigma}, \quad K_{lin} = \left(\frac{dF}{d\delta} \right)_{lin} \quad (1)$$

with: t_0 the initial assembly thickness, K_{lin} the slope of the linear section of the $\delta(F)$ curve, $\Sigma = \Sigma_0$ along the test.

To extract from E_{tot} the contribution of the insulated cable alone, we use the unidirectional rule of mixture for two components. In linear regime, the equivalent compressive modulus of the insulated cable E_c is given by (2):

$$E_c = \frac{v_c}{\frac{1}{E_{tot}} - \frac{1-v_c}{E_s}} \quad (2)$$

with: v_c the proportion of insulated cable in t_0 , $E_s = 85$ GPa.

This is a very much simplified mathematical model that should be taken with caution. For reasonable pressures (under 50 MPa), it gives correct orders of magnitude and it makes comparisons possible between the samples. From 50 MPa on, we observe large deformations of the samples implying Poisson effect. In these cases, we cannot use the rule of mixture anymore.

IV. RESULTS AND DISCUSSION

A. Bare Cable Characterization

Fig. 5 shows the compression curves of *LNI* and *RNI*. Both samples show a strong plastic behavior during the first compression ramps. This effect is interpreted as the plastic deformation of the copper cable braid. Visually, an important rearrangement of the cables is observed. Below 15 MPa, the behavior of both samples is similar. For higher pressures, *RNI* is much less deformed: around 3.5 % at 75 MPa versus 10 % for *LNI* at the same pressure. This confirms that the racetrack geometry improves the sample rigidity. Around 40 MPa, the compression curve of the ten-stack *LNI* shows a plateau which is the mark of a poor cohesion, due to the untwisting effect.

For both samples, after a first ramp to a given pressure, the behavior becomes quasi elastic. This can be considered as a mechanical training of the copper braid.

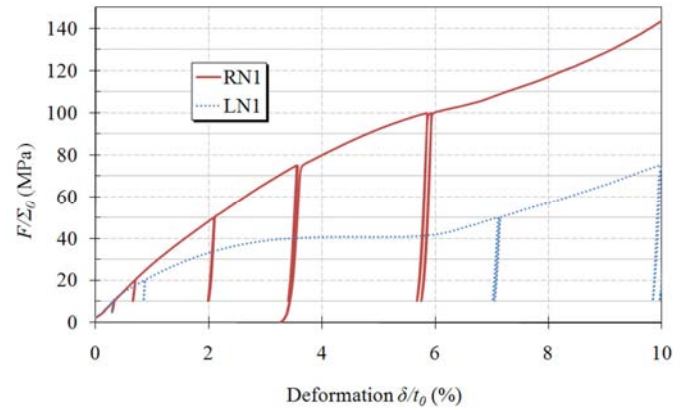


Fig. 5. Compression curves of *LNI* (till 75 MPa) and *RNI* (till 150 MPa).

B. Effect of the Insulation

Fig. 6 shows the compression curves of six samples, insulated or not. Their behavior is plastic during the first compression ramp and elastic during the following cycles for a given pressure. The effect of the cable training is dominant. The deformations of *LII*, *LI2* and *SII* are similar, with a plateau for pressures around 25 MPa. The test of *SII* has been stopped at 28 MPa because the untwisting was too important and the sample was ruined. Once again, it appears that the stack samples are not appropriate to reach large pressures with the cable we have. However, *RNI* and *RII* show no plateau. This demonstrates that the racetrack geometry improves the mechanical cohesion of the cables, either they are bare or insulated. The insulated samples are proportionally more deformed: at 75 MPa, *RII* shows a deformation of 6 % (3.5 % for *RNI*). This is due to the fact that the initial thickness of the insulated samples is larger.

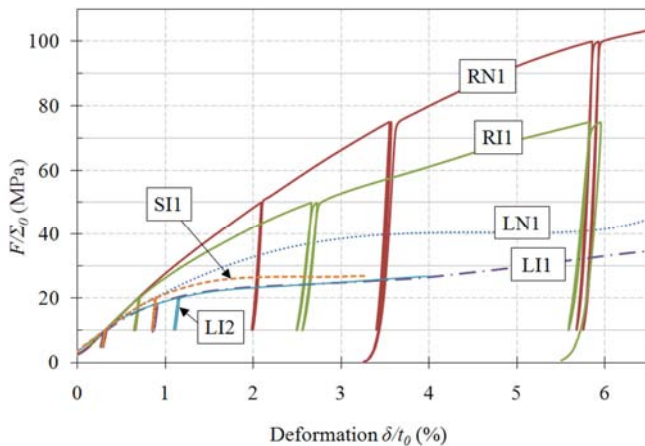


Fig. 6. Compression curves of *SII*, *LNI*, *LII*, *LI2*, *RNI*, and *RII*.

The equivalent compressive moduli E_c are computed in each elastic portion for the insulated samples, using the above-mentioned formulas. Fig. 7 gathers the results in a single plot, as a function of the test pressure, up to 50 MPa. The results are consistent between all types of samples. The moduli appear to be strongly pressure-dependant. This effect can be explained by the strands reorganization, affecting the sample rigidity. It is illustrated on Fig. 8 with *SII*, around 30 MPa.

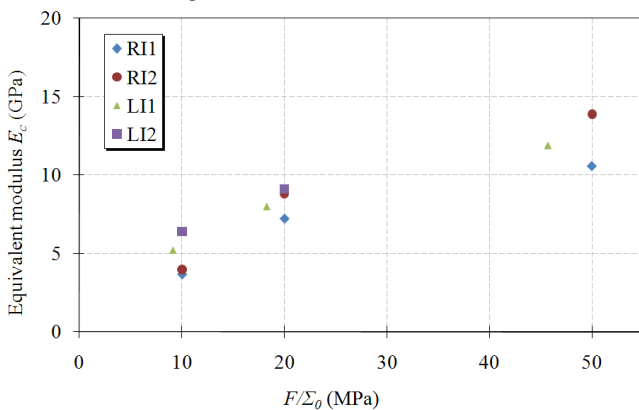


Fig. 7. Moduli of the insulated samples as a function of the test pressure.



Fig. 8. *SII* cross-section after compression till 30 MPa.

C. Contact Surface and Boundary Effects

For pressures above 50 MPa, the ceramic insulation mechanical properties are insufficient and cracks appear. This value seems low compared to the 65 MPa already achieved on the strand solenoids mentioned in part I. Due to the cable shape and to the absence of impregnation, the stress repartition on the sample is not homogeneous. The sensitive films show that the pressure concentrates in localized zones along the cables, inducing very large local stresses. Fig. 9 illustrates this remark on the sample *RI2* at 60 MPa. About 90 % of the

contact surface sees pressures higher than 10 MPa. But about 30 % of the surface reaches 130 MPa, which is more than twice the mean pressure. As expected, this ceramic insulation does not replace an epoxy impregnation. The lack of mechanical support in the composite cable generates large local stresses. Next step is to improve the way the space between strands is filled with the insulation.

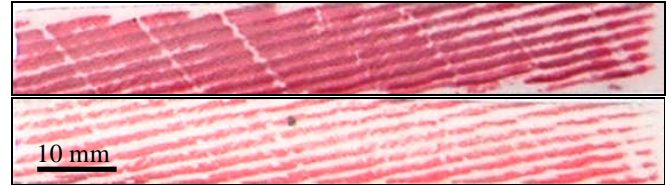


Fig. 9. Pressure-sensitive film on *RI2* after compression till 60 MPa. The film sensitivity ranges are: 10 to 50 MPa (top), and 130 to 300 MPa (bottom).

V. CONCLUSION

This study demonstrates the interest and the feasibility of the short racetrack samples for the mechanical characterization of ceramic-insulated cables. The mechanical results obtained in elastic regime are consistent with the results obtained with traditional cable stacks for pressures. For reasonable pressures (up to ~ 75 MPa), the cohesion of the sample is improved and the untwisting effect is reduced. For very high pressures, the sample loses cohesion and the insulation is ruined. The use of pressure-sensitive film shows that the stresses are concentrated in some areas.

The ceramic-insulated cable has supported compression tests up to 50 MPa with short racetrack samples, without visible degradation. The compressive modulus of the insulated cable is strongly dependant of the training pressure. The ceramic insulation is not able to sustain higher pressures in its present form. The next step is to improve the stress repartition inside the sample. This will be done by adapting the ceramic formulation and the deposition process in order to fill better the space, or by exploring the possibility of an impregnation material that would follow the heat treatment of the conductor.

ACKNOWLEDGMENT

The authors would like to thank Thomas Dalla-Foglia, Francis Pottier and Simon Saulnier for their technical support.

REFERENCES

- [1] A. Puigségur, F. Rondeaux, E. Prouzet, K. Samoogabalan, "Development of an innovative insulation for Nb₃Sn Wind & React coils," *Adv. Cryo. Eng. (Materials)*, vol. 50A, pp.266-272, 2004.
- [2] A. Puigségur, "Isolation céramique pour cables supraconducteurs Nb₃Sn," Ph.D. work presented in January 2005, CEA Saclay.
- [3] A. Puigségur, L. Quettier, J.M. Rey, F. Rondeaux, E. Prouzet, "An innovating insulation for Nb₃Sn wind & react coils: electrical tests," *IEEE Trans. on Applied Superconductivity*, vol. 16, Part 2, pp. 1769-1772(2006).
- [4] F. Rondeaux, L. Quettier, J.M. Rey, "Progress on an innovative insulation technique for Nb₃Sn wind & react coils," *Proceeding of ICEC22- ICMC2008*, pp 933-938.
- [5] F. Rondeaux, "Insulation development: final report on innovative insulation," *CARE Report*, 2007-037-NED, 2007.
- [6] A. Devred, et al., "Status of NED conductor development," presented at *IEEE/CSC & ESAS Europ. Superconductivity News Forum*, 2007, ST5.